J. of the Korean Sensors Society
Vol. 14, No. 4 (2005) pp. 225 – 230

Shaping of piezoelectric polyvinylidene fluoride polymer film for tip position sensing of a cantilever beam

Young-Sup Lee†

Abstract

This paper describes a novel tip position sensor made of a triangularly shaped piezoelectric PVDF (polyvinylidene fluoride) film for a cantilever beam. Due to the boundary condition of the cantilever beam and the spatial sensitivity function of the sensor, the charge output of the sensor is proportional to the tip position of the beam. Experimental results with the PVDF sensor were compared with those using two commercially available position sensors: an inductive sensor and an accelerometer. The resonance frequencies of the test beam, measured using the PVDF sensor, matched well with those measured with the two commercial sensors and the PVDF sensor also showed good coherence over wide frequency range, whereas the inductive sensor became poor above a certain frequency.

Key Words : PVDF film, spatial sensitivity, tip position sensor, cantilever beam, vibration control

1. Introduction

Conventional position sensors normally measure the motion of a point on a structure at a single position. There are several types of contacting and non-contacting position sensors that measure displacement e.g. LVDT (linearly variable differential transformer), ultrasonic distance sensors, optical sensors, and inductive proximity position sensors. These sensors have been widely used for the general measurement of displacement of structures. However, they are generally designed only to measure linear displacement over a limited range, and require a fixed point to attach to and are thus not suitable for slewing manipulators such as rotating beams. One of the best ways of measuring the tip position of rotational flexible beams is using a sensing device attached to or embedded in the beams. Possible devices could include distributed piezoelectric sensors, which could measure the integrated strain of a structure and could generate a charge output proportional to a tip position directly. Piezoelectric transducers have been widely used in various smart structures and mechanical systems[1,2]. The most commonly used piezoelectric materials in those smart structures are PZT (lead zirconate titanate) family for actuators and PVDF (polyvinylidene fluoride) polymer for sensors. The shaping of PVDF enables to develop specific sensors to detect important physical quantities of structural responses such as individual modal modes of a beam[3]. Apart from the distributed PVDF sensors, Burke and Hubbard[4] used a triangularly shaped piezoelectric device as an actuator on a simply supported beam for providing an overall moment excitation at one end of such a simply supported beam. In this paper, a new type of tip position sensor for a cantilever beam is described, which uses a triangularly shaped PVDF film. This sensor is distinguished from the modal sensors[4] in that it detects all the modal tip position without a summation process. Therefore, this new PVDF position sensor could be used for high precision tip displacement sensing of various cantilever beams.

2. Design of a PVDF position sensor

When an Euler-Bernoulli cantilever beam (length-width × thickness = $L_x \times L_y \times 2h_s$) is subject to flexural motion, the charge output $q(t)$ of a PVDF sensor bonded on the beam can be written as[5]

$$q(t)=\int_0^{L_x}\int_0^{L_y} S(x,y) \; h_{sen}\left[e_{31}\frac{\partial^2 w(x,y,t)}{\partial x^2}+e_{32}\frac{\partial^2 w(x,y,t)}{\partial y^2}\right]dxdy\,, \qquad (1)$$

Principal Researcher, Korea Research Institute of Standards and Science
†Corresponding author: yslee@kriss.re.kr
(Received : January 13, 2005, Accepted : March 2, 2005)

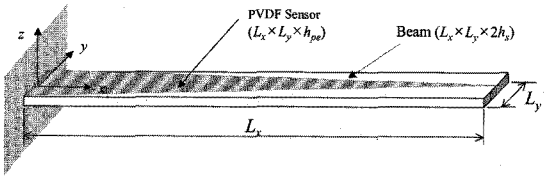

Fig. 1. A triangularly shaped piezoelectric sensor bonded on one side of a cantilever beam.

where e_{31} and e_{32} are the piezoelectric stress constants, h_{sen} is the distance between the neutral axis of the beam and the PVDF sensor, and $w(x, y, t)$ is the two-dimensional displacement of the beam. If the beam is assumed to be one-dimensional ($L_x >> L_y$) then Eq. (1) can be rewritten as

$$q(t)=e_{31}h_{sen}L_y\int_0^{L_x} S(x,t)\frac{\partial^2 w(x,t)}{\partial x^2}dx\,. \tag{2}$$

A triangular shaped PVDF sensor ($L_x \times L_y \times h_{pe}$) bonded on a cantilever beam is considered as shown in Fig. 1, the spatial sensitivity function $S(x, y)$ of the sensor can be defined for $x = 0$ to L_x

$$S(x,t)=-k(x-L_x)\,, \tag{3}$$

where $k=L_y/L_x$ is the slope of the triangular sensor. Eq. (2) can be expressed as

$$q(t)=e_{31}h_{sen}L_y \left\{\left[S(x,t)\frac{\partial w(x,t)}{\partial x}\right]_0^{L_x}-\frac{\partial S(x,t)}{\partial x}\int_0^{L_x}\frac{\partial w(x,t)}{\partial x}dx\right\}, \tag{4}$$

where $\partial S(x,t)/\partial x$ is a constant and Eq. (2) is expanded so that

$$q(t)=e_{31}h_{sen}L_y\left\{\left[S(L_y,y)\frac{\partial w(L_x,t)}{\partial x}\right]-\left[S(0,y)\frac{\partial w(0,t)}{\partial x}\right] -\frac{\partial S(x,t)}{\partial x}[w(L_x,t)-w(0,y)]\right\}. \tag{5}$$

Since the spatial sensitivity $S(x,t)$ with the triangular shaped sensor has the following conditions:

$$S(0,y)=kL_x,\ S(L_x,y)=0,\ \text{and}\ \frac{\partial S(x,y)}{\partial x}=-k \tag{6}$$

and the boundary conditions are given by $w(0,t)=0$ and $\frac{\partial w(0,t)}{\partial x}=0$, Eq. (5) becomes

$$q(t)=e_{31}h_{sen}L_y k w(L_x,t)\,, \tag{7}$$

where $w(L_x,t)$ is the flexural tip position of the cantilever beam. Thus the tip position $w(L_x,t)$ of a cantilever beam can be expressed by

$$w(L_x,t)=\frac{q(t)}{e_{31}h_{sen}kL_y} \tag{8}$$

This triangular PVDF sensor can have $q(t)$ proportional to the tip deflection of a cantilever beam.

3. Experimental Set-up

A triangular shaped PVDF position sensors has been built (isosceles triangular type) and it was bonded on a cantilever beam. The physical properties of the steel beam were $L_x \times L_y \times 2h_s$=300 × 20 × 1 mm and the thickness of the PVDF sensor was h_{pe} = 52 μm, and the constant k in Eq. (3) is 1/15. Two commercially available position sensors have been used in the experiment together with the PVDF sensor. As shown in Fig. 2, the two commercial sensors are an inductive proximity sensor (Honeywell proximity sensor 924 series 30 mm) and an accelerometer (B&K Type 4393), which were located at the beam's tip.

The frequency responses $T_R = w(L_x)/f(x_a)$ were measured in the experiment, where $w(L_x)$ is the displacement at the tip of the beam and $f(x_a)$ is the input force applied on a location x_a of the beam. The force $f(x_a)$ is generated by a shaker (Ling Dynamic Systems model V101) and has been measured with a force transducer (B&K Type

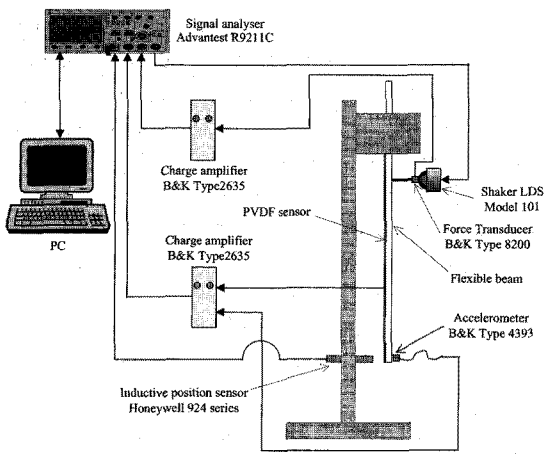

Fig. 2. Experimental set-up.

8200) which is connected to a spectrum analyser (Advantest R9211C FFT analyser) via a charge amplifier (B&K Type 2635).

The shaker location x_a was about 90 mm away from the clamped end of the beam. The inductive proximity sensor was connected to the spectrum analyser directly and the accelerometer was connected to the spectrum analyser via a charge amplifier (B&K Type 2635). The two commercial sensors were located centrally on the beam, at the tip, as shown in Fig. 2.

The sensitivity of the piezoelectric film was taken into account in calculating the absolute displacement per unit force for the PVDF sensors to compare with the results from the other sensor

4. Results and Discussion

Fig. 3 shows the measured frequency response function of the PVDF sensor (thick line) is compared with the proximity sensor (thin dashed line), the accelerometer (thin line) and the calculated beam response (thick dashed line) over frequency range of 0-1000 Hz as shown in Fig. 3. Fig. 3 shows the measured magnitude and phase responses with respect to the input signal against frequency. The peaks due to the first, second, third, fourth, and sixth bending modes are clearly seen.

Since the "fifth resonance", at around 550 Hz, is overlapped with the anti-resonance, the fifth resonance is not plotted clearly. This is also confirmed from the calculated response with a theoretical beam model with a tip mass, which is based on the model of Laura *et al.*[6].

Considering the results below 300 Hz, Fig. 3 shows that the PVDF sensor has the largest output, the accelerometer is the next, and the inductive proximity sensor is the smallest at the same input force. This is because the inductive proximity sensor has a diameter of 30 mm which is bigger than the width of the beam (20 mm), so that the measured location was not exactly at the tip of the beam.

The measured locations by the inductive sensor and the accelerometer were near the tip. In contrast to the two commercial sensors, the triangularly shaped PVDF sensors can measure exactly the behaviour at the tip of the beam. The calculated response from a theoretical beam model suggests that the response measured by the accelerometer is the most similar to the calculated response among the three different sensors. The

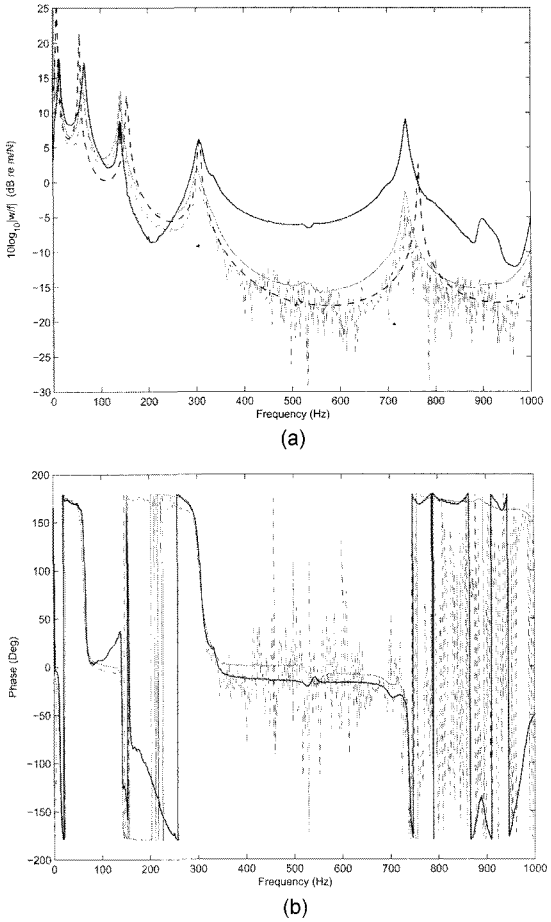

Fig. 3. Measured frequency response function; (a): magnitude and (b) phase of the sensor.

responses of the PVDF sensor showed good coherence as well. Above 500 Hz there is clearly a difference between the magnitudes of the response from the triangular PVDF sensor and that from the accelerometer. This could be because the PVDF sensor is exposed to torsional motion. However, in practice we would like to obtain a charge output proportional only to the flexural motion of a beam. This could be achieved with a small k, which makes the sensor narrower compared with the beam width. Lee and Moon[3] showed the response of piezo sensors was sensitive to small errors in the shapes of the transducers, particularly affecting the high frequency response. In order to demonstrate the effect, another steel cantilever beam of $L_x \times L_y \times 2h_s = 200 \times 30 \times 1$ mm with a triangularly shaped PVDF sensor of $h_{pe} = 0.5$ mm was built as shown in Fig. 4.

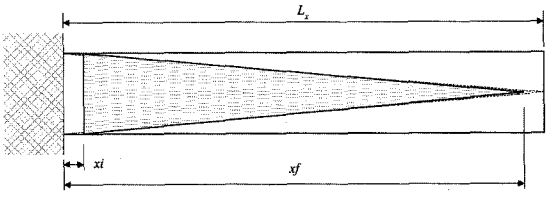

Fig. 4. A simulation model of a triangularly shaped PVDF sensor with shaping error.

The PVDF sensor was made so that the base was about 2 mm away from the clamped end of the beam. Assuming a tip point force $F_i(t)$ excites the beam, then the charge output is expressed as

$$q(\omega)=e_{31}h_{sen}L_y\sum_{n=1}^{\infty}B_n(\omega)\int_0^{L_x}S(x,y)\frac{\partial^2\phi_n(x)}{\partial x^2}dx \qquad (9)$$

where $B_n(\omega)$, $\phi_n(x)$, ω_{on}, ρ_s, A_s, and η_s are the harmonic modal amplitude, mode shape, natural frequency, density, sectional area, and loss factor of the beam. Considering the sensitivity function $\hat{S}(x)$ of the PVDF sensor with shaping errors, the harmonic mobility[7] response can be written as

$$\hat{T}(\omega)=j\omega\frac{\hat{q}(\omega)}{F_i(\omega)}=\frac{j\omega e_{31}h_{sen}L_y}{\rho_s A_s L_x}\sum_{n=1}^{\infty}\frac{\phi_n(L_x)\int_0^{L_x}\hat{S}(x,y)\frac{\partial^2\phi_n(x)}{\partial x^2}dx}{[\omega_{on}^2(1+j\eta_s)-\omega^2]} \qquad (10)$$

The integration in Eq. (10) is the source of shaping error because it can not satisfy the boundary conditions in Eq. (6). That is $\hat{S}(0,y)\neq kL_x$ and $\partial\hat{S}(x,y)/\partial x\neq -k$ for $0\le x\le L_x$. Thus the integration result of Eq. (9) becomes, using partial integration, as

$$\hat{q}(t)=e_{31}h_{sen}L_y\left\{\left[\hat{S}(x,t)\frac{\partial w(x,t)}{\partial x}\right]_0^{L_x}-\int_0^{L_x}\frac{\partial\hat{S}(x,y)}{\partial x}\frac{\partial w(x,t)}{\partial x}dx\right\}$$
$$\neq e_{31}kh_{sen}L_y w(L_x). \qquad (11)$$

A computer simulation based on Eq. (10) has been performed when the beam is subjected to a tip force. The simulation model uses the geometry of the sensor illustrated in Fig. 4, where $L_x=200$ mm, xi and xf are both the distances from the clamped end of the beam to both ends of the sensor. Fig. 5 shows the responses with shaping errors when xi varies and $xf=L_x$, in which the thin line represents the exact shape, the dashed and dotted line is for $x_i=1$ mm, the dashed line is for $x_i=5$ mm, and thick line is for $x_i=10$ mm. The measured resonance frequencies are almost unaffected but the anti-resonance frequencies are different from each other or even disappeared. This is because excessive xi can detect additional charge output which is of opposite sign compared with the charge output with an exact shape. The charge output of a sensor with shaping error xi can be expressed with

$$\hat{q}(t)=e_{31}h_{sen}L_y\left\{\left[\hat{S}(L_y,y)\frac{\partial w(x,t)}{\partial x}\Big|_{x=L_x}\right]-\left[\hat{S}(xi,y)\frac{\partial w(x,t)}{\partial x}\Big|_{x=xi}\right]+\hat{k}[w(L_x)-w(xi)]\right\}$$
$$=q(t)+q_{add}(t), \qquad (12)$$

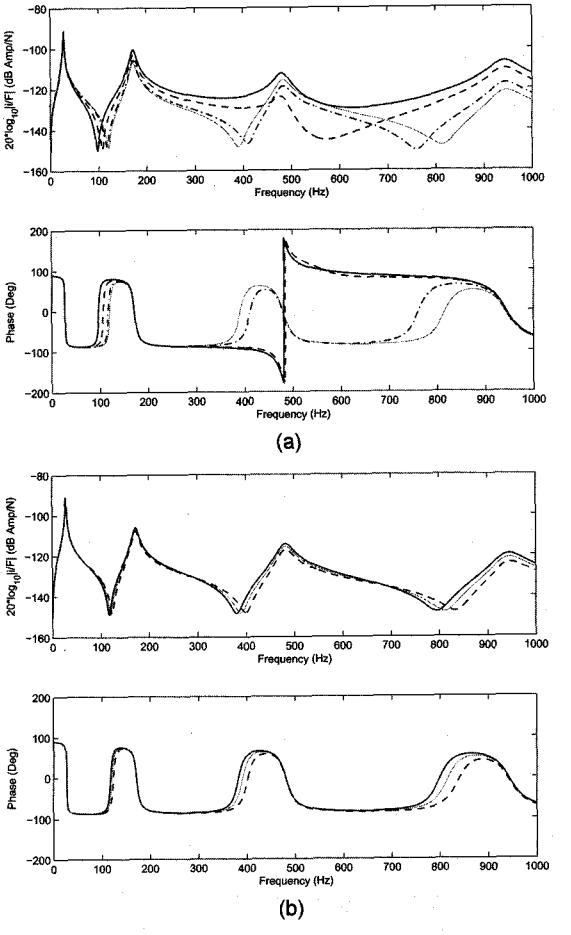

Fig. 5. Effects of shaping errors; (a) Shaping error due to xi and (b) Shaping error due to xf.

where $\hat{S}(L_y,y)=0$, and the slope of the sensor $\hat{k}=L_y/(L_x-xi)$, and the additional charge output $q_{add}(t)$ due to shaping error is given by

$$q_{add}(t)=e_{31}h_{sen}L_y\left\{-\hat{S}(xi,y)\frac{\partial w(x,t)}{\partial x}\bigg|_{x=xi}-\hat{k}w(xi)\right\}. \quad (13)$$

With an exact shape, the sensor will generate $q(t)$ only. However, $\hat{q}(t)$ can become a different sign compared with that of in Eq. (13), when $|q_{add}(t)|>|q(t)|$. The sign changes at the third and the fourth modes in Fig. 5 are caused by excessive xi. So a small xi such as 1 mm could not change the sign, as shown in Fig. 5, because of small $q_{add}(t)$ compared with $q(t)$. Fig. 5 shows the responses with shaping errors when xf varies and $xi=0$, in which thin line represents $Lx-xf=0$ for exact shape, dashed line is for $Lx-xf=5$ mm, and thick line is for $Lx-xf=-5$ mm. The effect by xf is not bigger than that by but becomes to increase with frequency. The presence of xf represents that the sensor measures not the beam's tip displacement but the displacement of the location at xf away from the beam's tip. Hence, assessing from the simulation results, the shaping error of the PVDF sensor at the clamped end of the beam is more serious than that at the tip.

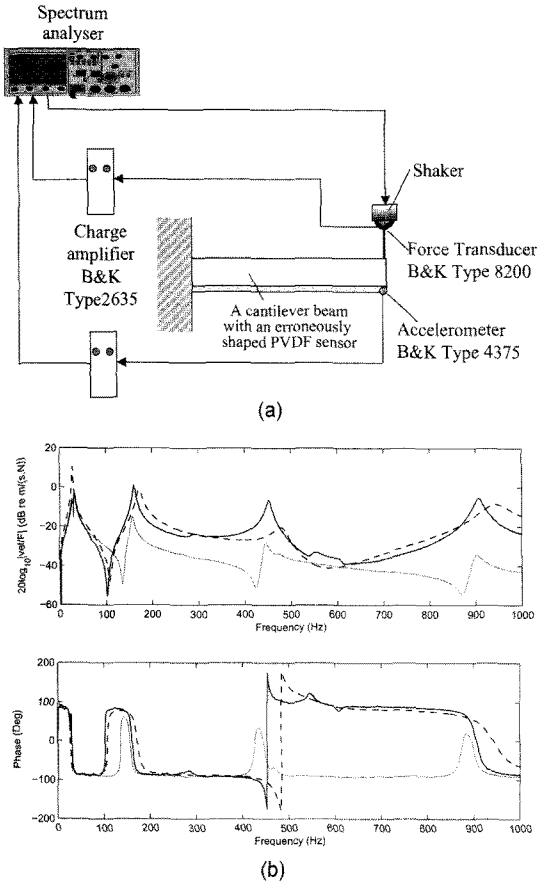

Fig. 6. Measured shaping error effect; (a) Measurement set-up for a cantilever beam with an erroneously shaped PVDF sensor and (b) Shaping error effects in measurement.

Another experimental measurement was made with the actual PVDF sensor bonded on the beam with the erroneously shaped PVDF sensor when a shaker excites the beam vertically at the tip as shown in Fig. 6. The input force signal was measured from a force transducer (B&K Type 8200) via a signal conditioner (B&K Type 2635 charge amplifier) and the charge outputs from the PVDF sensor and an accelerometer (B&K Type 4375) were detected using the experimental set-up. The harmonic current output $i(\omega)$ (the time derivative of the charge output $q(\omega)$) taken from the erroneously shaped PVDF sensor, has been measured. The experimental responses and the simulation results with the erroneously shaped sensor are compared in Fig. 6 (right). The thin line in Fig. 6 represents a typical feature with a shaker and an accelerometer. The resonances are alternated by anti-resonances occurred at frequencies quite close to the following resonance. Also the phase response lies between $\pm 90^{\circ}$ and the amplitude tends to decrease with frequency[8].

However, the thick line indicates the measured response with a shaker and the PVDF sensor and shows the 2nd, 3rd and 4th resonances are excessively large compared with the shaker and an accelerometer response. It also can be seen that the first and the second modes are detected as minimum phase responses but the third and the fourth are not. The computer simulation results with a shaker and the erroneous PVDF sensor (thick dashed line) when $xi=5$ mm shows a very similar trend with the measured ones. The origin of this mismatching between the two responses was the shaping error of the PVDF sensor. Shaping errors should thus be minimized for triangular PVDF sensors in order to detect the tip position of cantilever beams.

Thus the triangular shaped PVDF film can be used as an error sensor for active cancellation systems of sound and vibration[9].

5. Conclusions

A novel tip position sensor made of a distributed piezoelectric PVDF film for a cantilever beam has been described in this paper. The position sensor was designed based on the electro-mechanical property of the piezoelectric transducers piezoelectric to generate charge output proportional to the tip displacement of a cantilever beam when the beam is subject to purely flexural motion. The relationship between the tip displacement of a cantilever beam and the charge output of the PVDF sensor has been derived.

The experimental result with the triangular PVDF sensor was compared with two commercially available position sensors: an inductive sensor and an accelerometer (after double integration). The resonance frequencies of the test beam picked up by the PVDF sensor was well-matched with the two commercial sensors and the PVDF sensor showed very good coherence in wide frequency range, whereas the inductive sensor became very bad after 300 Hz. Also The effect of shaping errors in PVDF sensors has been discussed in depth, with theoretical and experimental verification.

References

[1] C. R. Fuller, S. J. Elliott, and P. A. Nelson, "Active control of vibration", Academic Press, London, 1996.

[2] R. L. Clark, W. R. Saunders, and G. P. Gibbs, "Adaptive structures dynamics and control", John Wiley & Sons, New York, 1998.

[3] C. K. Lee and F. C. Moon, "Modal sensor/actuators", *ASME Journal of Applied Mechanics*, vol. 57, pp. 434-441, 1990.

[4] S. E. Burke and J. E. Hubbard Jr., "Active vibration control of a simply supported beam using a spatially distributed actuator", *IEEE Control Systems Magazine*, pp. 25-30, 1987.

[5] C. K. Lee, "Theory of laminated piezoelectric plates for the design of distributed sensors/actuators. Part I: Governing equations and reciprocal relationships", *Journal of Acoustical Society of America*, vol. 87, no. 3, pp. 1144-1158, 1990.

[6] P. A. A. Laura, J. L. Pombo, and E. A. Susemihl, "A note on the vibrations of a clamped-free beam with a mass at the free end", *Journal of Sound and Vibration*, vol. 37, no. 2, pp. 161-168, 1974.

[7] L. Cremer and M. Heckl, "Structure-borne sound (2nd Edition)", Springer-Verlag, Berlin, 1988.

[8] D. J. Ewins, "Modal testing: theory and practice", John Wiley & Sons, New York, 1984.

[9] J.-I. Sohn, M. Lee, and W. Lee, "Active noise cancellation using a teacher forced BSS learning algorithm", *Journal of The Korean Sensors Society*, vol. 13, no. 3, pp. 224-229, 2004.

이 영 섭

- 1987 부산대학교 공과대학 조선공학과 학사
- 1997 영국 사우샘턴대 음향진동연구소 (ISVR) 석사
- 2000 영국 사우샘턴대 음향진동연구소 (ISVR) 박사
- 2001 영국 사우샘턴대 음향진동연구소 (ISVR) Research Fellow
- 2003 한국표준과학연구원 스마트계측그룹 책임연구원
- 주관심 분야 : 압전 센서/액추에이터, 스마트구조 음향/진동 능동제어 및 신호처리